Investigating the role of porous pebbles as vehicles for gas transport from the protoplanetary disk onto the surface of an accreting planet

Emrik Conradzon

Division of Astrophysics
Department of Physics

LUND UNIVERSITY

2026-EXA257

Degree project of 15 higher education credits
June 2026

Supervisor: Anders Johansen

Division of Astrophysics
Department of Physics
Box 118
SE-221 00 Lund
Sweden

Abstract

The pebble accretion scenario has been proposed as an alternative to the classical theory of planet formation via planetesimal core accretion. In this alternative scenario, once the rocky cores of planets exceed a certain threshold, the mass evolution of planetary embryos are thought to be driven through the accretion of small aggregates of dust grains, which form in the protoplanetary disk, called pebbles. This theory solves several problems within the classical scenario; primarily, that planets forming via core accretion must accrete mass on a time scale much longer than is feasible, while planets forming via pebble accretion gain masses comparable to those within the solar system, crucially on a timescale falling within the lifetime of the protoplanetary disk. Secondly, while the core accretion scenario accurately describes the masses of some planets within the solar system, the rate of mass accretion drops sharply with stellar distance, necessitating untenable assumptions about the column density of the protoplanetary disk in order to explain the masses of the farther planets such as Uranus and Neptune.

In this project we reproduce a 1D model of planetary formation via pebble accretion. We assume in this model that the pebbles are silicates and investigate their sublimation and survival-rates as they move through the protoplanetary envelope. By making use of a dimensionless filling factor, describing the solid volume fraction of the pebbles, we assume that the corresponding fraction of the volume of these pebbles is taken up by stellar gases within the pores of the mineral. We then use the sublimation temperature of (forsterite) silicates in order to predict the amounts of gas from these inclusions that are deposited into the magma ocean on the surface of the planet. Our goal is to investigate whether this mechanism may be a viable candidate for explaining the discrepancies between the isotopic compositions of four representative noble gas isotopes found within the sun and within the earth's mantle. The results point to the model overestimating the delivery of the light ^{22}Ne isotope, while under-delivering the three heavier ^{36}Ar, ^{84}Kr and ^{130}Xe isotopes compared to survey measurements of the terrestrial surface and atmospheric inventories. Interpreting the results of the project as a proof-of-concept for the model of gas accretion into the protoplanetary core, the over-delivery of ^{22}Ne shows that even by this simplified model there will likely be a meaningful contribution of gaseous material to the core material within the pebble accretion scenario.

Glossary

- **PPD** - Protoplanetary Disk.
- **Hill radius,** R_H = Region of space where gravity of a central mass dominates.
- **Bondi radius,** R_B = distance from the central mass where the escape velocity is equal to the sound speed of the medium.
- **Scale height,** H = Distance over which a quantity decreases by a factor of e.
- **Envelope** = A primordial layer of gas and dust surrounding a protoplanetary embryo; behaves like a highly diffuse atmosphere bound by the embryo's gravity.
- **Core accretion** = Classical planet formation model in which planetary cores grow through successive collisions and sticking of pre-existing planetesimals.
- **Sublimation** = Phase transition in which a solid directly becomes a gas without passing through a liquid phase.
- **Dust** = Primordial solid grains in a protoplanetary disk, typically $\sim 1\,\mu$m in size; also referred to as monomers or grains.
- **Fragmentation barrier** = Growth limit where collisions between pebbles occur at high relative velocities, leading to fragmentation instead of sticking and halting further growth.
- **Bouncing barrier** = Growth limit where low-mass grains collide but rebound rather than stick, preventing efficient coagulation into larger aggregates.
- **Radial drift barrier** = Process in which intermediate-sized solids rapidly lose angular momentum due to gas drag and drift inward toward the star before they can grow further.
- **Streaming instability** = Collective effect arising from interaction between solid particles and gas in a protoplanetary disk, where local concentration of solids reduces relative drift, producing dense filaments that can gravitationally collapse into planetesimals.
- **Isotope** = Variant of an element characterized by a different number of neutrons while retaining the same number of protons.
- **Fractionation** = Process that separates a previously homogeneous material into distinct fractions based on physical or chemical differences, such as mass-dependent isotopic separation.

Popular Science Description

What are planets made out of? How do they form? What makes Mars a small, rocky, planet and Jupiter a large gaseous planet? Questions like these have been fascinating us since before we formed ways of writing them down. Sumerians studied planets movements across the skies in hopes to interpret messages from the gods, Plato imagined the planets marked the boundaries between different 'spheres' of existence itself, and Sir Isaac Newton used their paths across the skies to infer the universal nature of gravity.

To this day, the open question of how planets form continues to be a topic of ongoing discussion. While we now have a better understanding of the processes which play a part in planetary formation, there are still many question-marks which need straightening out. Our current best understanding of how planets are formed is centered around what is known as the core accretion scenario, where large asteroids called '*planetesimals*' zip around a large disk of ice, dust, and gas which forms around a young star known as the '*protoplanetary disk*' (PPD).

As these planetesimals move around, they crash into one another and collect dust until they are massive enough to bind an '*envelope*' of gas, akin to a more diffuse atmosphere, around them. This envelope functions as a drag-net around the protoplanet, and as it moves through the PPD the friction between the dust in the medium and the envelope may help it accrete even more mass.

The research question we are trying to answer with this project is whether these dust grain-coagulates, or '*pebbles*' as they are more commonly known, may themselves contain small pockets of gas which could then be dragged down into the forming planet as it accretes mass. If this is so, then pebble accretion may be the mechanism behind a previously unexplained phenomenon; why we see such similarities between the isotopic signatures of noble gases, found here on Earth, and within the Sun. If these gases were transported into the rocky core of the planet via more massive meteorites, then the concentrations would favor the heavier isotopes. We also know that the envelopes around protoplanets exchange some gas with the PPD, but we still have yet to explain the mechanism by which these gases from within the PPD are transported into the rocky cores of forming protoplanets.

Contents

1 Introduction

In recent years the pebble accretion model has been introduced as a supplement to the classical core accretion scenario of planetary formation theory. In the standard model of planetary formation, core accretion is considered (cf. Armitage (2017)) as the only mechanism by which planets gain mass. However, this does not explain the evolution of the planetary mass within the life-time of the protoplanetary disk (PPD), and additionally, it can not provide an explanation for the fate of the large amounts of dust particles observed in the disks around young accreting stars (Zsom et al. 2010). The pebble accretion model revolves around the accretion of pebbles, micrometer- to centimeter-sized coagulates of dust within the PPD, as the main driver behind planetary mass accretion.

For the purposes of this project the pebbles are assumed to be coagulates of refractory silicate monomers, and we investigate their sublimation behavior as they move through the envelope. The main goal of the project was to investigate whether these pebbles, which coagulate from dust in the PPD, may contain inclusions of primordial gas. If the pebbles survive the journey through the hot inner layers of the planetary envelope, they may deposit this gas into the magmatic ocean of the planet. This could serve to explain the discrepancies between the isotopic composition of terrestrial gases and those observed within the sun, and specifically whether these gases may be transported into the planetary core via this pebble accretion mechanism. Taking the abundances of the solar protoplanetary disk presented by Lodders (2003) as representative of the concentrations of, for example, noble gases within the protoplanetary disk, we model the flux and cumulative mass delivered of isotopes of four noble gases over the growth time of the accreting protoplanet. Beyond this point in time, the disk dissipates, and as the pebbles no longer are driven inward by the radial gas flow, pebble accretion ceases to be a viable growth mechanism. The isotopes of the four noble gases included in this model are ^{22}Ne, ^{36}Ar, ^{84}Kr and ^{130}Xe, as these were highlighted as representative isotopes by Marty (2012) for the open question of what planet forming mechanisms play a role in determining geochemical abundances.

The results of the model show that while pebble accretion-assisted delivery of disk gas over-delivers the lighter element ^{22}Ne, the heavier isotopes of ^{36}Ar, ^{84}Kr and ^{130}Xe are not accreted efficiently enough to explain the comparative terrestrial inventories laid out in Marty (2012). This implies the possibility that ^{22}Ne may be delivered efficiently by the pebble accretion mechanism, while the heavier noble gas inventories likely stem from a contribution of carbonaceous chondrites which are known to contain significant abundances of trapped heavy noble gases and have previously been proposed (cf. Marty (2012)) as a source of Earth's volatile inventory.

2 Theory

2.1 The protoplanetary disk. (PPD): The protoplanetary disk forms as a consequence of the collapse of a solar nebula into a young star. The remaining gas and dust compact onto the central star due to gravity, which attenuates the inherent random movements of the particles in favor of the directional plane of the net angular momentum, whereby it gains its characteristic disk geometry. As the temperature of the disk declines with distance slower than the gravitational influence of the star, there exists a hydrostatic equilibrium between the gradient of gas pressure and the disk-orthogonal component of stellar gravity which causes the disk to flare at larger radii. The ratio between the sound speed c_s and the Keplerian frequency Ω_k can therefore be used to define the fundamentally useful *scale height*, $H(r)$, to assess conditions within the PPD at a given point. As the disk material redistributes its angular momentum, the turbulent conditions can be described by an effective viscosity ν which can be approximated as a time-independent power-law function of the radius (e.g. Hartmann et al. (1998) ; Armitage (2017)). Following the works of Shakura and Sunyaev (1973), which characterize the efficacy of angular momentum transfer by the dimensionless parameter α, the viscosity can be written in terms of the local scale height and sound speed as

$$\nu = \alpha c_\mathrm{s} H. \tag{1}$$

The mass accretion rates of PPDs have been used to determine α to be in the range of 10^{-2} to 10^{-4} (cf. Manara et al. (2023)). Although recent studies indicate that the value of α may not be homogeneous throughout the entirety of the disk (Lesur et al. (2014)), this inhomogeneity presents mainly between vertical layers of the disk. We may therefore safely take α to be constant, as planetary formation takes place within the mid-plane of the PPD. This higher $\alpha = 10^{-2}$ represents a high amount of turbulence in the PPD relative to the lower value of 10^{-4}, which hinders the coagulation of solids within the disk. Taking a constant value of α represents a homogeneity between the vertical layers of the disk. Such a homogeneity is not likely to be found in a physical protoplanetary disk. However, as taking the upper bound of $\alpha = 10^{-2}$ limits dust settling and the growth of solids, this simplification represents a conservative assumption. A more realistic, vertically varying α, with lower turbulence near the mid-plane of the disk would likely promote more efficient coagulation of solids and planet formation than predicted in this implementation of the model.

Recent surveys of the protoplanetary disk sizes performed using the Atacama Large Millimeter/submillimeter Array (ALMA) (e.g. Long et al. (2019)) show that while Class II protoplanetary disks are commonly found to have sizes between $\simeq 40$ to 200 AU, sizes above 100 AU are rare ($\simeq 15\%$). Following the model outlined in Steinmeyer et al. (2023), we take for our disk size a radius $R_1 = 90\,\mathrm{AU}$. The temperature profile of the disk can be described by a radial power law (Steinmeyer et al. (2023))

$$T(a) = 150 \left(\frac{a}{\mathrm{AU}}\right)^{-\zeta} \mathrm{K} \tag{2}$$

dependent on the distance a to the central star. This description is not accurate in all parts of the disk, however, as described by e.g. Mori et al. (2021), the temperature in the inner parts of the

disk is dominated by stellar irradiation and thus Steinmeyer et al. (2023) choses to neglect the effects of viscous heating.
Making use of the pebble accretion model from Johansen et al. (2019), Steinmeyer et al. (2023) then argues that one can describe the disk aspect ratio with the power law

$$\frac{H}{a} \propto \left(\frac{a}{\mathrm{AU}}\right)^{-\zeta/2+1/2}. \tag{3}$$

The sound speed, normally obtained by the scale height and the Keplerian frequency Ω_k as $c_s = H\Omega_k$, then is similarly described by a power law as

$$c_\mathrm{s} \;=\; H\Omega \;=\; c_{\mathrm{s},0}\left(\frac{a}{\mathrm{AU}}\right)^{-\zeta/2}, \tag{4}$$

where c_{s0} is the sound speed $650\,ms^{-1}$ taken at $1\ \mathrm{AU}$. Basing our framework from the model as implemented in Steinmeyer et al. (2023), we take the negative logarithmic temperature gradient to be $\zeta = 3/7$ for the irradiated disk model.

2.2 Pebble formation and PPD mass budget.: Surveys of protoplanetary disks (e.g Bergin et al. (2013)) find disk masses in the range between 1% to 10% of the central stellar mass. However, this quantity is notoriously difficult to measure as the main mass-component of stellar disks is $\mathrm{H_2}$ which does not display millimeter transitions. By integrating the dust- and gas-surface densities from the $\mathrm{CO}-\mathrm{dust}$ line, Franceschi, Riccardo et al. (2022) gain estimates of disk masses for a near-solar mass star (the $\mathrm{TW\ Hya}$-disk) on the order of $\simeq\ 0.11\mathrm{M}_\odot$. As the disk evolves, the infall of gas and dust into the inner regions of the disk will effectively lower the available mass budget for planetary formation.

The dust grain sizes in the early stages of the PPD evolution are generally found to be a function of the degree of turbulence within the disk, expressed in terms of α, as the turbulence induces collisions between solid grains and places constraints on their growth by effectively determining the maximum size coagulates may attain before collisions between pebbles become destructive rather than adhesive. A representative value of the mean physical size of dust grains in the early disk is often taken as $r_\mathrm{dust} = 1\mu\mathrm{m}$ (Drażkowska et al. (2019)). Using this size and the drag force experienced by dust particles one may define their dimensionless aerodynamical sizes ; the Stokes number St of the particle by computing the stopping time τ_stop, the timescale at which a particle with mass m and velocity Δv relative to the surrounding gas slows down (Armitage (2017)). Defining St as multiplying this with the Keplerian frequency Ω_k at the given distance to the central star, a, we are left with a dimensionless expression for the size of frictionally coupled solids within the disk,

$$\mathrm{St} = \Omega \times \tau. \tag{5}$$

As gas is gravitationally attracted to the central star, and aerodynamically small solids within the disk couple strongly to the motion of the gas, the turbulence within the disk due to e.g. self-gravity, magnetohydrodynamic effects (Lesur et al. (2014) ; Armitage (2017)) and the streaming instability (Johansen and Youdin (2007)), transports and redistributes angular momentum and, crucially for the present work, gives rise to collisions between disk solids (Okuzumi et al. (2012)) in which dust particles may collide and stick (Drażkowska et al. (2019) ; Mori et al. (2021)) to form pebbles. While these solids (which we refer to within this thesis equally as monomers, dust particles or grains) drift radially inwards due to frictional interaction with the slow-moving disk gas, they collide and adhere to one another to form pebbles (equally referred to as coagulates or aggregates). This growth of pebbles through collisions between solids in the PPD is hindered by three barriers, the *fragmentation* barrier where the velocities of the particles is high enough that collisions between solids lead to fragmentation, resupplying the disk with small sized grains, the *bouncing* barrier describes the tendency of low-mass grains to bounce off one another with little to no mass transfer and the *radial drift* barrier which describes how intermediate sized particles ($\mathrm{St} \simeq 1$) display the most efficient drift behavior and often reach the star before growing (Zsom et al. (2010) ; Birnstiel et al. (2016)).

To overcome these barriers and form planetesimals the mechanism known as *streaming instability* has been proposed as a solution by Johansen et al. (2007). The streaming instability (*SI*) was found analytically by Youdin and Goodman (2005) and subsequently confirmed numerically by several groups (e.g. Johansen and Youdin (2007) ; Simon et al. (2016); Schäfer et al. (2017)). This mechanism arises through the interplay between the radial drift speed of particles and the ratio between solid-to-gas density, as the solids exert a drag force on the surrounding gas. Clusters of solids create a local bump in the density of particles frictionally interacting with the gas which attenuates the orbital speed of the gas to be close to Keplerian (Schäfer et al. (2017)), which causes a reduction in the drift speed of solids locally. This creates areas of solid densities, which have been found to be high enough to undergo gravitational collapse and form planetesimals from particle clusters containing as much mass as 3.5 times the mass of the dwarf planet Ceres (Johansen et al. (2007)), roughly 4×10^{21} kg, or $0.055\ \%$ of $\mathrm{M}_{\oplus}$. An illustrative representation of how the streaming instability expedites the formation of planetesimals within the PPD is shown in figure (1).

2.3 Planetary Core formation.: Core accretion via planetesimals has been extensively described, and therefore we neglect to include a full description in this work, while noting that in the classical theory the protoplanetary core grows via collisions of similar sized planetesimals. During times where the mass of the protoplanetary core is lower than a mass threshold, denoted the mass of pebble accretion onset, M_{PA} (Johansen and Lyra (2026)), the core only ineffectively captures pebbles from the surrounding disk as the majority of solids are aerodynamically deflected (Visser and Ormel (2016)) and its gravitational influence is not high enough to contract an envelope (Johansen and Lambrechts (2017)).
While planetesimal collisions require huge timescales to form planetary cores of masses comparable to the core masses of gas giants Armitage (2017), they may still form protoplanets which surpass above the initial mass threshold, M_{PA}.

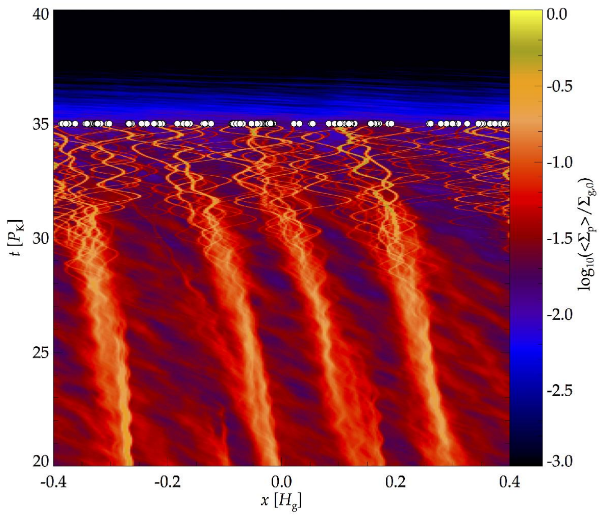

Figure 1: Illustration showcasing the effects of the streaming instability (SI). The pebble column density, Σ_{peb}, is integrated in the vertical direction within the disk and averaged over the azimuthal. The color-mapping (specified on the right edge in the figure) shows the logarithmic density ratio over time on the vertical axis. Figure collected with permission from Schäfer et al. (2017).

2.4 Protoplanetary envelope development.: Once the protoplanet has grown to a sufficiently high mass, PPD gas in its vicinity will become gravitationally bound. The extent of the neighborhood within which gas is gravitationally bound to the protoplanetary embryo is denoted the Bondi radius, R_B, and is a function of the protoplanetary mass M_p, equivalent to the point at which the sound speed of the gas is equal to the escape velocity from the protoplanetary core, given as

$$R_B = \frac{G\mu M_\mathrm{p}}{k_\mathrm{B}T} = \frac{GM_\mathrm{p}}{c_\mathrm{s}^2}. \tag{6}$$

Within the Bondi radius, the gas contracts and forms a gaseous envelope around the core. Typically, low-mass planets contract envelopes that are in hydrostatic equilibrium with its surroundings in the PPD (cf. Kippenhahn et al. (2012) ; Drazkowska et al. (2022)). As the outer envelope drops in temperature via the radiative cooling, the gas contracts onto the planet and more gas from the nearby disk will take its place, thus leading to an increase in the envelope mass and in its size proportional to the cooling and contraction timescale of the envelope. This is the Kelvin-Helmholtz thermal timescale which describes the upper limit of the amount of gas that a planet can bind as being strongly coupled to the opacity of the envelope and the protoplanetary mass. The opacity of the envelope is, as described by e.g Bell and Lin (1994), closely linked to the temperature and density of the envelope, as a low opacity hinders the envelope from cooling via radiative emission. Radiation and convection are the two most important methods of energy transfer within the protoplanetary envelope. While a portion of its energy is lost through radiation, the gas drag of incident solids from the disk, along with their deposition of potential energy near the core, will heat the envelope enough to sustain it Lambrechts et al. (2014). An illustration showing the envelope formation and development is included in figure (2). Through these accretion- and

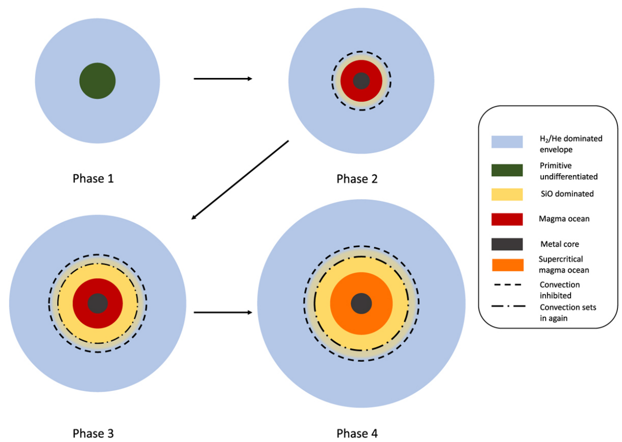

Figure 2: Illustration showing the phases of the planet during its formation process, and the adhering layers within the envelope. In Phase 1, a $\mathrm{H_2/He}$ rich envelope forms around the protoplanetary core which extends up to the Bondi radius R_B (eq. 6). Phase 2 initiates as the core differentiates into a metallic core surrounded by a magma ocean on the surface. In Phase 3, the aforementioned SiO-convective layer manifests, obstructing the opacity of the envelope. In Phase 4 the temperature of the protoplanet becomes so intense that the magma ocean becomes supercritical. Figure collected and included with permission from Steinmeyer and Johansen (2024).

radiative processes, the luminosity L of the planet can be expressed a function of the accretion rate $\dot{M}$ onto the planet, given in Steinmeyer et al. (2023) on the form

$$L = G \times \frac{M_\mathrm{p}\,\dot{M}}{R_p}. \tag{7}$$

2.5 Noble gases as geochemical tracers.: The goal of this project is creating a model of planet formation via pebble accretion, and by estimating the volume of gas each pebble drags down into the convective inner SiO-layer (Steinmeyer and Johansen (2024)), to calculate the amounts of a number of elements delivered to the protoplanetary core during the lifetime of the PPD. By calculating these amounts, using tabulated elemental and isotopic primordial inventories presented by Lodders (2003), and comparing to the measured atmospheric (ATM) and bulk mantle (BM) concentrations of select stable noble gases taken from Marty (2012), we produce cumulative and specific accretion histories over these isotopes for an Earth analogue.

As noble gases are chemically inert, atmophile, incompatible during silicate partial melting (Avice et al. (2022)), and crucially all have at least one or more non-radiogenic isotopes, they are the best and most readily available geochemical tracers of the geophysical developmental history and are thus a salient keystone in investigating the planetary formation process. The isotopic composition of noble gases within the Earth is often viewed as a key constraint on its formational history. Specifically, the isotopic compositions of Ne and Xe on Earth stand out in comparison to the other terrestrial planets (Ozima and Podosek (2001)). The $^{20}\mathrm{Ne}/^{22}\mathrm{Ne}$ ratios measured of the Earths mantle reveal a reduction in ^{20}Ne relative to atmospheric Ne. This result has been taken as suggesting that the outgassing and the atmospheric escape of primordial Ne may be sensitive to mass-dependent fractionation (cf. Sect. [**7.2**] in Ozima and Podosek (2001)). However, Marty (2012) argues that this kind of hydrodynamic escape would impact the isotopic signatures of other stable volatile elements, instead positing that an alternative explanation for this discrepancy could be that the origins of primordial Ne are, as of yet, too poorly understood, and could be result of mixing between two or more cosmochemical end-members ; carbonaceous chondrites and gas-rich meteorites. Geochemical analyses of meteorites and carbonaceous chondrites have consistently shown (cf. Black and Pepin (1969) ; Marty (2012)) higher ^{20}Ne/^{22}Ne ratios in gas-rich meteorites ($\approx 12 - 14$) than in carbonaceous chondrites ($\simeq 8.2 - 9.2$). In this project we investigate the viability of porous pebble-driven gas accretion to the protoplanetary core as a possible explanation for the isotopic composition of the core of an Earth-analogue.

3 Accretion Model

To determine the accretion rates of noble gases from within the PPD we follow the model of planet formation via pebble accretion outlined in e.g Johansen et al. (2019), Steinmeyer et al. (2023) to model the circumstances of the planet growth which sets boundaries on the pebble and gas flux. This model takes the development history of the disk and the migration of the planet into account.

3.1 PPD initial conditions: To calculate the growth track of the accreting protoplanet, we assume the PPD follows a classic α-disk model where the turbulent viscosity is given by

$$\nu = \alpha c_s H. \tag{8}$$

Typical α-values of Solar System-analogous PPD's were determined by Mulders et al. (2017) to be in the range 10^{-4} to 10^{-2}. We take for our model $\alpha = 10^{-2}$. Mori et al. (2021) used a magnetohydrodynamical model of a typical protoplanetary disk to show that the temperature profile of the inner disk is largely determined by the radiation of the star, whereby the Johansen et al. (2019) model opts to neglect the effects of viscous heating and describes the radial temperature profile of the disk as a power-law, given in (eq. 2).

3.2 Planetary parameters: Within the pebble accretion model described in Johansen et al. (2019) the growth rate, $\dot{M}$, of the planet is given as a function

$$\dot{M} = 2\left(\frac{\mathrm{St}}{0.1}\right)^{2/3} \Omega R_{\mathrm{H}}^2 \Sigma_{\mathrm{p}}, \tag{9}$$

such that the planet mass M increases proportionally with the Stokes number St as in (eq. 5) of the pebbles and the surface density, Σ_{p}, of solids in the disk. To avoid the explicit computation of the interaction time between the pebbles and the envelope within the Hill radius, R_{H}, we instead use the equivalent expression of $\dot{M}$ from Steinmeyer et al. (2023) which gives the mass growth rate in terms of the gas mass accretion rate $\dot{M}_g(t)$ at a given time and distance a to the central star, expressed as

$$\dot{M} = 2\times\left(\frac{St}{0.1}\right)^{2/3} \sqrt{GM_*}(3M_*)^{-2/3}\times\frac{\xi\dot{M}_g(t)}{2\pi\left[\chi St\ + (3/2)\alpha\right] c_{s,0}^2 AU^{-\zeta}} M^{2/3}\left(\frac{a}{AU}\right)^{(\zeta-1)}. \quad (10)$$

This growth rate is also dependent on a number of derived parameters. The stokes number St describes the aerodynamical sizes of solids, and the ratio ξ between solid-to-gas-mass flux as material accretes onto the star

$$\xi = \frac{\dot{M}_p}{\dot{M}_g}. \quad (11)$$

The negative logarithmic pressure gradient in the disk χ is given as $\chi = \beta + \zeta/2 + 3/2$ where β and ζ are the negative logarithmic derivatives of the gas surface density and temperature profiles, respectively. While mass of the planet M_{P} is in the range of $0.001 - 0.01\ M_{\oplus}$, the pebble accretion is said to take place in the Bondi regime, where the incident velocities of pebbles are set by the sub-Keplerian motion of the PPD gas. The streaming instability may create planetesimals with masses within this range (Johansen et al. (2007)), but the low rates of pebble accretion due to aerodynamic deflection in the Bondi regime (where the stopping time due to gas drag forces becomes shorter than the timescale at which solids pass the Bondi sphere (Visser and Ormel (2016))) serve as a hindrance to producing protoplanetary cores above $M_{\mathrm{PA,\,init}}$ unless aided by planetesimal core accretion. Johansen and Lambrechts (2017) show that in the early stages of protoplanetary core formation, the column densities of planetesimals are sufficient to create cores that can reliably overcome this barrier. Once the planetary embryo has reached $\geq 0.01\ M_{\oplus}$ the Hill radius given by

$$R_{\mathrm{H}} = a\left(\frac{M_{\mathrm{P}}}{3M_*}\right)^{(1/3)} \quad (12)$$

becomes larger than the R_{B}. In this *Hill regime*, where $R_H \geq R_{\mathrm{B}}$, the gravitational influence of the core on passing pebbles within the disk is strong enough to the point where the viscosity of the surrounding disk is affected to such a degree that the approach velocity of pebbles becomes effectively set by the Keplerian shear. From this point onward the efficiency of pebble accretion becomes sufficiently high to where Johansen et al. (2019) argue that one may safely ignore the accretion of planetesimals within their model. In spite of the low accretion efficiency below $0.01\ M_{\oplus}$, we take for our model an initial planetary mass of $0.001\ M_{\oplus}$ as we assume a constant gas-to-solid-density flux in the disk which sets the pebble accretion rate onto the planet. This assumed relation is reasonable as long as we rely on the assumption that the density of planetesimals is high in the early stages of our planetary core's development (based on the conclusions of e.g Johansen et al. (2019) ; Johansen et al. (2015)).

The radius of the protoplanet with mass M_{p} is given by

$$R_{\mathrm{p}} = \left(\frac{3M_{\mathrm{p}}}{4\pi\rho_{\mathrm{p}}}\right)^{1/3} \quad (13)$$

where ρ_p is the density of the planet, which we take to equal the density of the uncompressed Earth, found by Hughes (2006), $\rho_\mathrm{p} = 4050\,\mathrm{kg\ m^{-3}}$.

3.3 Planet Migration: The model computes the migration (type-I) of the planet as a function of its mass as

$$a(M) = a_0 \left(1 - \frac{M^{4/3} - M_0^{4/3}}{M_\mathrm{max}^{4/3} - M_0^{4/3}}\right)^{1/(1-\zeta)} \tag{14}$$

where M_0 and a_0 are the initial mass and stellar distance, respectively. The parameter M_max represents the mass that the planet would accrete if it migrated from its initial position a_0 down to $a = 0$; this projection is described by Johansen et al. (2019) as a scaling law

$$M_\mathrm{max} = 11.7\,M_e \left(\frac{(\mathrm{St}/0.01)^{1/2}}{[(2/3)(\mathrm{St}/\alpha)/\chi + 1]/2.9}\right)^{3/4} \left(\frac{\xi}{0.01}\right)^{3/4} \left(\frac{M_*}{M_\odot}\right)^{1/4} \times \left(\frac{k_\mathrm{mig}}{4.42}\right)^{-3/4} \left(\frac{c_{\mathrm{s},0}}{650\ \mathrm{m\ s^{-1}}}\right)^{3/2} \left(\frac{1-\zeta}{4/7}\right)^{-1} \left(\frac{a_0}{25\ \mathrm{AU}}\right)^{(3/4)(1-\zeta)}. \tag{15}$$

The prefactor k_mig appears when analytically solving for the shape of type-I migratory tracks, and depends on the negative logarithmic derivative of the surface density and temperature profile, but is taken to be a constant as these phenomena are included elsewhere in the model (Johansen et al. (2019)). The model also takes into account the evolution of the gas mass accretion rate onto the central star $\dot{M}_\mathrm{g}(t)$ expressed by Hartmann et al. (1998) as

$$\dot{M}_\mathrm{g}(t) = \dot{M}_0 \left(\frac{t}{t_\mathrm{s}} + 1\right)^{(-(5/2-\gamma)/(2-\gamma)} \tag{16}$$

where $\gamma = 3/2 - \zeta$ is the coefficient such that the viscosity in the disk follows $\nu \propto r^\gamma$. The characteristic timescale t_s for a disk with initial disk size R_d0 where $\nu = \nu_{R(\mathrm{d0})}$, given by

$$t_s = \frac{1}{3(2-\gamma)^2} \frac{R_\mathrm{d0}^2}{\nu_{R(\mathrm{d0})}}. \tag{17}$$

The gas surface density Σ_g is set by the gas accretion rate onto the central star

$$\dot{M}_g = -2\pi r u_r \Sigma_g, \tag{18}$$

where u_r is the accretion speed of the gas at a given point within the mid-plane of the disk such that

$$u_r - \frac{3}{2}\frac{\nu}{a} = -\frac{3}{2}\alpha c_s \frac{H}{a}. \tag{19}$$

Initial conditions used for our application of the model, taken from Steinmeyer et al. (2023) are presented in table 1.

Using a fourth-order Runge-Kutta method to integrate equation (10) over the considered time

Table 1: Initial conditions and parameters used in this iteration of the model. These values were gathered from Steinmeyer et al. (2023), save for $R_{\rm peb}$ which is discussed in (eq. (20 ; 21).

Symbol	Description	Value
a_0	Starting position	1.985 AU
M_0	Starting planetary mass	$10^{-3}\ M_\oplus$
t_0	Starting time	3.5×10^6yr
$\dot{M}_{\rm g,0}$	Initial gas accretion rate	$10^{-7}\ M_\odot\ \ {\rm yr}^{-1}$
$\dot{M}_{\rm g,1}$	Final gas accretion rate	$10^{-9} M_\odot\ {\rm yr}^{-1}$
$t_{\rm D}$	Life-time of PPD	5×10^6 yr
ξ	Pebble-to-gas flux ratio	0.003
St	Stokes number	0.01
ζ	Logarithmic derivative of T	$3/7$
β	Logarithmic derivative of $\Sigma_{\rm g}$	$15/14$
$R_{\rm d0}$	Initial disk size	90 AU
$R_{\rm peb}$	Pebble Geometric Size	1 cm

period within which an inner planet starting at position a_0 and ending at Earth's position $a = 1\,{\rm AU}$ within the disk $t_{\rm D} - t_0 = 3.5$ Myr, we solve for the mass accretion and migration by equation 14 in parallel results in the growth track presented in figure 3 overleaf. In order to solve for the growth track we assume a constant solid-to-gas-mass flux ratio ξ of 0.003. As the pebble accretion efficiency in the Hill regime and the radial drift of pebbles both depend on the aerodynamical properties of the pebbles, we define their size by the Stokes number St which is set at 0.01. Assuming silicate pebbles of $\rho_{\rm peb} = 3000\ {\rm kg\ m^{-3}}$ and an initial gas mass accretion rate of $\dot{\rm M}_{\rm g}\ = 10^{-7}\ {\rm M}_\odot\ {\rm yr}^{-1}$, this corresponds to

$$\mathrm{St} = \sqrt{2\pi} \times \frac{3\pi\,\nu\,\mathrm{R_{peb}}}{\dot{\mathrm{M}}_{\rm g}}, \tag{20}$$

implying a physical pebble size $R_{\rm peb}$ of

$$R_{\rm peb} = \frac{\mathrm{St}}{\alpha}\,\frac{\dot{\mathrm{M}}_{\rm g}}{\sqrt{2\pi}\,3\pi\,\nu\,c_{\rm s} H \rho_{\rm peb}}. \tag{21}$$

As we define $\mathrm{St} \equiv 0.01$, this implies pebble sizes $R_{\rm peb} \approx 1.7{\rm cm}$. To simplify the computations, we account for the diminishing $\dot{M}_{\rm g}$ over $t_{\rm D}$ when calculating $R_{\rm peb}$ by using an average of the pebble sizes, letting $R_{\rm peb} \equiv 1$ cm, as their sizes shrink to $\simeq 0.8$ cm as $\dot{M}_{\rm g} \to 10^{-9}\ M_\odot\ {\rm yr}^{-1}$. Beginning the evolution of the $0.001 M_\oplus$ mass planet at a distance of $a_0\ = 1.985$ AU, our planet accretes about $0.68\ M_\oplus$ over the course of 1.5 Myr and migrates down to a distance $a = 1$ AU. Beyond this point, after the disk has dissipated, mass accumulation via pebble accretion becomes ineffective, as no radially flowing gas exists to facilitate their migration. However, there is good evidence that some amount of planetesimal core accretion takes place after the disk has dissipated (Johansen et al. (2015)), and a moon-forming giant impact takes place somewhere around $40\,{\rm Myr}$

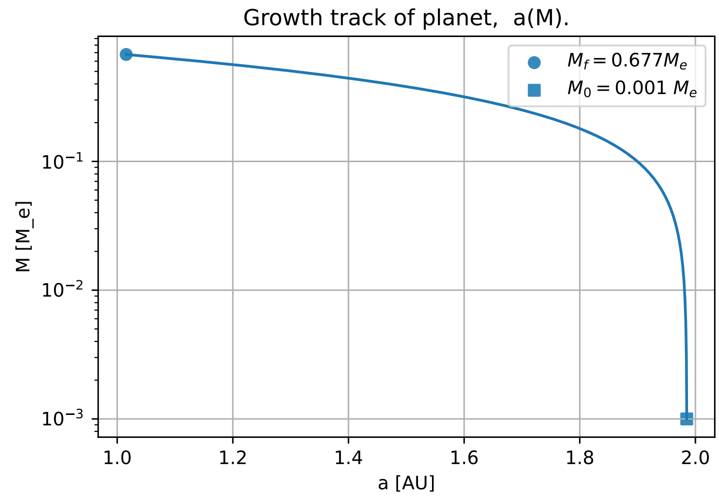

Figure 3: Growth track of the planet between t_0 and the life-time of the disk, $t_{\rm D}$. Its initial position in the disk is at $a_0\ = 1.985{\rm AU}$, marked by a square, and it proceeds down to $a = 1.0\ AU$, accreting a total mass of $\simeq 0.68 M_\oplus$, which is marked in the plot by a circle. Beyond this point where $t \geq t_D$, the disk dissipates and pebble accretion ceases.

after the end of the disk lifetime (Lock et al. (2018) ; Yu and Jacobsen (2011) ; Johansen, Anders et al. (2023)), we claim that the planet produced by the model can be treated as an Earth analog (Steinmeyer et al. (2023)).

3.4 Envelope structure development: Had the lifetime of the disk been longer, pebble accretion would continue until the planet reached an isolation mass $M_{\rm iso}$ above which, in the wake of its orbit, it would trace a ring shaped gap within the disk. The edges of the annulus represent locally reversed pressure gradients, which act as barriers for radially migrating solids within the PPD (Drazkowska et al. (2022)). The magnitude of $M_{\rm iso}$ is determined largely from the assumed viscosity of the disk, via the α parameter, and Lambrechts et al. (2014) obtain $M_{\rm iso}$ on the order of $20\,M_\oplus$ whereas Drazkowska et al. (2022) argue that this value for a solar-like PPD is likely closer to $\simeq\ 25\ M_\oplus$. Were our planet to approach this isolation mass, the surrounding envelope would contract as a consequence of the discontinued heating by the gas friction of in-falling pebbles, and a denser, structured, atmosphere would begin to form.

As the planet accretes mass on a very long timescale compared to the radial gas accretion rate, we may safely conclude that the equations of hydrodynamical equilibrium between the envelope and the surrounding disk apply throughout the entire growth process. By assuming a spherically symmetric envelope in hydrodynamic equilibrium with the surrounding disk, the standard structure equations described by cf. Kippenhahn et al. (2012) adequately model the envelope structure.

We therefore solve the mass conservation-, hydrostatic balance- and thermal gradient equations

$$\frac{\mathrm{d}m}{\mathrm{d}r} = 4\pi r^2 \rho, \tag{22a}$$
$$\frac{\mathrm{d}P}{\mathrm{d}r} = -\frac{GM}{r^2}\rho, \tag{22b}$$
$$\frac{\mathrm{d}T}{\mathrm{d}r} = \nabla \frac{T}{P}\frac{\mathrm{d}P}{\mathrm{d}r}, \tag{22c}$$

from the outermost point of the envelope down to the planetary core. The edge of the envelope, r_{out}, is taken to be the Hill radius R_{H}, as outside the Hill sphere the radial flow of gas towards the central star outweigh the gravitational influence of the planet and the conditions needed to solve these equations no longer apply (Steinmeyer et al. (2023)). We therefore take r to be the point in the envelope such that $R_{\mathrm{p}} \leq r \leq R_{\mathrm{H}}$, and let ρ, T and P be the density, temperature and pressure of the envelope at each point r, respectively.

The boundary value for the temperature, T_{out}, is found by equation 2, and we assume an ideal gas corresponding to a proto-solar hydrogen gas/helium mixture with mean molecular weight of $2.34\,m_{\mathrm{u}}$, as given by Lodders (2003), an adiabatic index ς of 1.4 was chosen as in (cf. Steinmeyer et al. (2023)). The energy transport within the envelope occurs mainly through radiation, when the opacity is sufficiently low, and convection when the density of solids in the envelope is high enough that radiation is quickly reabsorbed. The model separates these layers of the envelope via the temperature gradient ∇, defining this in the radiative region as

$$\nabla_{\mathrm{rad}} \equiv \frac{\kappa(T)P}{64\pi G M_{\mathrm{p}} \sigma T^4} L, \tag{23}$$

where σ is the Boltzmann constant, L is the luminosity of the planet described in 7 and $\kappa(T)$ is the opacity as a function of the temperature, which is taken to be a broken power law using the parameters $\kappa_i,\ a_i,\ b_i$ from Bell and Lin (1994) such that

$$\kappa = \kappa_i \rho^{a_i} T^{b_i}. \tag{24}$$

In this expression, the $\kappa, a,$ and b parameters are given different values depending on the main source of opacity in the regime considered (cf. Bell and Lin (1994)) and as in Steinmeyer et al. (2023) we assume the three main sources contributing to the opacity within the envelope are ice grains, metal grains and gas molecules.

While this ∇_{rad} is smaller than the corresponding *adiabatic* temperature gradient ∇_{ad}, the envelope is assumed to be effectively transparent to radiation. Where $\nabla_{\mathrm{rad}} > \nabla_{\mathrm{ad}}$, defined as

$$\nabla_{\mathrm{ad}} \equiv \frac{\varsigma - 1}{\varsigma}, \tag{25}$$

convection will occur. We therefore let ∇ in equation 22c be the minimum value between

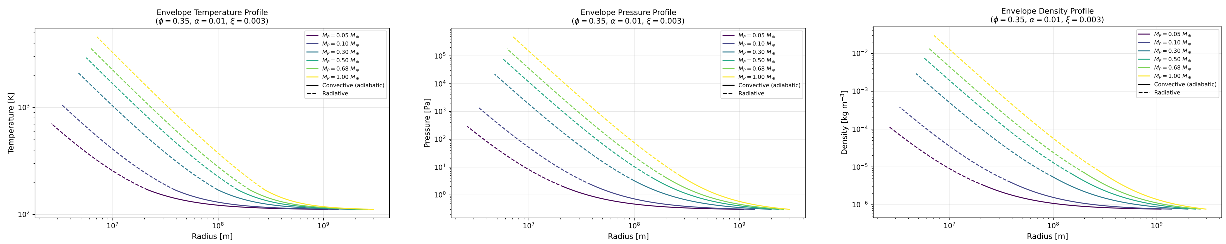

Figure 4: Combined envelope profiles for temperature, pressure, and density across different masses. Areas where the envelope is convective or radiative are marked out with filled and dashed linestyles, respectively.

∇_{ad} , ∇_{rad} when computing the thermal profile of the envelope. To obtain a boundary value for the pressure in the envelope with which to solve the coupled differential equations in (eq. 22), we assume the disk gas is an ideal gas, where $T_{\rm out}$ is the temperature given by (eq. 2), such that the pressure obeys

$$P_{\rm out} = \frac{\rho_{\rm d}}{\mu m_{\rm u}} k_{\rm B}\, T_{\rm out}. \tag{26}$$

Choosing to look at silicate pebbles composed of forsterite ($\mathrm{Mg_2SiO_4}$), as enstatite ($\mathrm{MgSiO_3}$) is a common ultra-refractory mineral within protoplanetary disks (Steinmeyer et al. (2023)), which produces a protective layer of forsterite gas during its sublimation, we take the sublimation temperature T_S of the pebbles equal to that of forsterite. In reality, the sublimation temperature of a solid j is a function of the supersaturation level S_j, where solids sublimate at a rate that is dependent on the partial pressures and stoichiometric coefficients of the reactants and products in the reactions. Put simply; to correctly model the sublimation of pebbles composed of a single mineral would require more precise modeling of the entire chemical makeup and the Gibbs free energy ΔG of the reactants and their products.

In this simplified model iteration we assume that once the pebbles pass beyond a nominal sublimation temperature of $T_S(\mathrm{Mg_2SiO_4}) \simeq 1500$ K, pebbles are effectively fully accreted and deposit their full mass into the magmatic ocean, whether immediately or after a period of settling (cf. Ormel (2014) ; Visser and Ormel (2016); Mordasini, C. (2014)). Simulations by Ormel et al. (2015) have shown that the envelope exchanges gas with the surrounding disk through recycling flows. These penetrate as deep as the Bondi radius of the planet. We do not take these recycling flows into account, which could be a way that the planet loses some of the specific gas which is delivered with the pebbles. We motivate our disregarding of this mechanism by two arguments; Firstly, the Bondi radius for planet masses in the range $(0.01 - 0.68\ M_\oplus)$ manifests itself far outside the point in the envelope where the temperature reaches the T_S of silicates (cf. Fig. **5** in Steinmeyer et al. (2023)), even at very low pressures. Secondly, since we are not accounting for the chemical evolution of the disk gas, these recycling flows would contain the same natural abundances as the accreted gas and hence our results would not change without including the changes to the chemical concentrations of the nearby disk material over $t_{\rm D}$.

3.5 Pebble Structure: A singular, exact, astrophysical definition of a pebble as used in this context does not exist, and depending on the hydrodynamical conditions of the disk are where the pebbles are formed greatly impact their qualities (e.g. size, porosity, geochemical composition). What is common between models is that pebbles are taken to be coagulates of dust grains from within the PPD. These monomers collide and stick to one another to form larger structures (Zsom et al. (2010)) which are then denoted pebbles. The majority of solid monomers in PPD, found via sub-millimeter spectroscopy in surveys of PPD around low-mass $\mathrm{T-Tauri}$ stars (e.g. Hartmann et al. (1998)) and ALMA/VLA multi-wavelength surveys (Jiang, Haochang et al. (2024)) have observed grain-sizes ranging between $0.1\mu\mathrm{m} - 1\mathrm{mm}$ (Long et al. (2019)).

Fluids within the disk have a high adsorption cross-section in interactions with the surfaces of monomers (Öberg and Bergin (2021)), meaning that the surfaces of grains within the disk often are covered in e.g. water vapor. Outside the snow-lines, this leads to the build-up of ice on the surface of grains which improves their sticking efficiency (Gonzalez and Michoulier (2026)). This mechanism also aids in the production of large planetesimals via the streaming instability (see e.g. Johansen et al. (2007) ; Okuzumi et al. (2012)). When these icy grains collide and stick, they form porous coagulates (Michoulier et al. (2024)) whose combined volumes may exceed that of its constituents (Okuzumi et al. (2012)), due to the formation of enclosed cavities. These cavities are in contact with the surrounding disk material, and thus the pebbles will contain a certain volume of gas which could exceeds its solid volume (Zsom et al. (2010)). The porosity of pebbles is not currently well understood, and many researchers are currently working on modeling how the porosity of pebbles manifests in different areas of the protoplanetary disk and drag regimes (Gonzalez and Michoulier (2026) ; Schneider, Niclas and Wurm, Gerhard (2021)). To approximate the volume of gas contained within each pebble, we use the filling factor ϕ (Zsom et al. (2010) ; Blum and Schräpler (2004) ; Michoulier et al. (2024)), which is a dimensionless parameterization of the solid volume fraction of the pebbles, where the V_{total} is given by, $V = (4\pi/3)\pi R^3$ taking R_{peb} from (eq. 21), is given by

$$\phi = \frac{V_{\mathrm{solid}}}{V_{\mathrm{total}}}. \tag{27}$$

Depending on the amount of turbulence within the disk, which drag regimes (Stokes, Epstein) are considered, and the sticking efficiency of monomers, ϕ has been found by Michoulier et al. (2024) to be as small as on the order of 10^{-3} when considering a seeding process of ice covered grains beyond the CO snow-line, while Blum and Wurm (2008) find ϕ in the range $(10^{-2} - 0.35)$ depending largely on the relative velocities of solids in the disk. As these aggregates collide and stick to one another, however, some degree of compactification will occur as a consequence of the impact energy dispersion in the two coagulates (Okuzumi et al. (2012)). In order to simplify our calculations we use a nominal value of $\phi = 0.35$, which Zsom et al. (2010) specify as an "*intermediate* porosity", as compared to a *high* porosity of $\phi = 0.15$. However, we present results for the accretion of the heavy ^{22}Ne isotope for a range of $\phi \in (0.01 - 0.5)$. We do not compute the accretion histories of the four noble gases considered for each ϕ in this range.

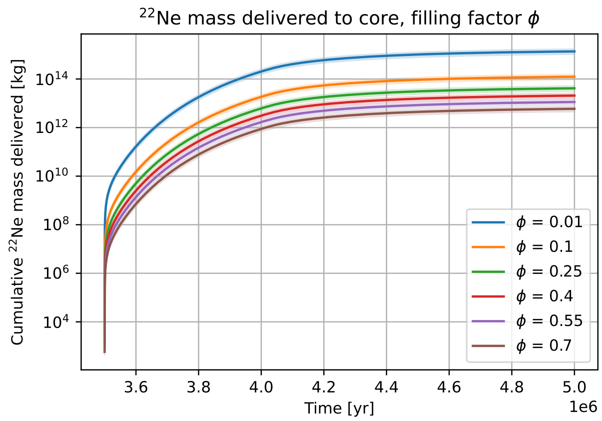

Figure 5: The cumulative amounts of ^{22}Ne delivered during the $3.5\,\text{Ma}$ accretion time for different filling factors ϕ in the range $\phi \in (0.01 - 0.7)$.

Without accounting for the chemical evolution of the disk gas or the various processes (e.g. atmospheric escape or mantle degassing) that depend on mass fractionation, the cumulative accretion of all four isotopes would increase with the same linear proportionality to ϕ.

3.6 Calculating the pebble flux: By utilizing (eq. 10), and assuming only pebbles contribute to the mass growth rate of the planet, we make use of the chosen ϕ and R_{peb} to calculate the solid mass held within each pebble as

$$m_{\text{peb}} = \rho_{\text{peb}}\,(\phi \times V_{\text{tot}}), \tag{28}$$

by taking $\rho_{\text{peb}} = 3000\,\text{kg}\,\text{m}^{-3}$ for forsterite (Steinmeyer et al. (2023)). Comparing the m_{peb} to the growth rate yields the number of flux of pebbles for each point in time in the planets formation history. This number flux is then used to calculate the gas delivery each pebble contributes with as it is accreted. Solving the coupled differential equations (eq. 22a-22c) to gain the pressure within the envelope at the point where the temperature reaches $T_S(\text{Mg}_2\text{SiO}_4) = 1500$ K, then the pressure yields the density of the envelope as

$$\rho_{\text{env}} = P(T_S)\frac{\mu}{k_b T_S}. \tag{29}$$

Making use of the gas volume fraction of each pebble $V_{\text{gas}} = V_{\text{tot}}(1-\phi)$, the density of the envelope gas where $T = T_S(\text{Mg}_2\text{SiO}_4)$, we then calculate the mass of delivered gas. We make no attempt at accounting for outgassing or escape of fluids from within the envelope, and assume that once a pebble passes this threshold, its contents are deposited into the core of the planet.

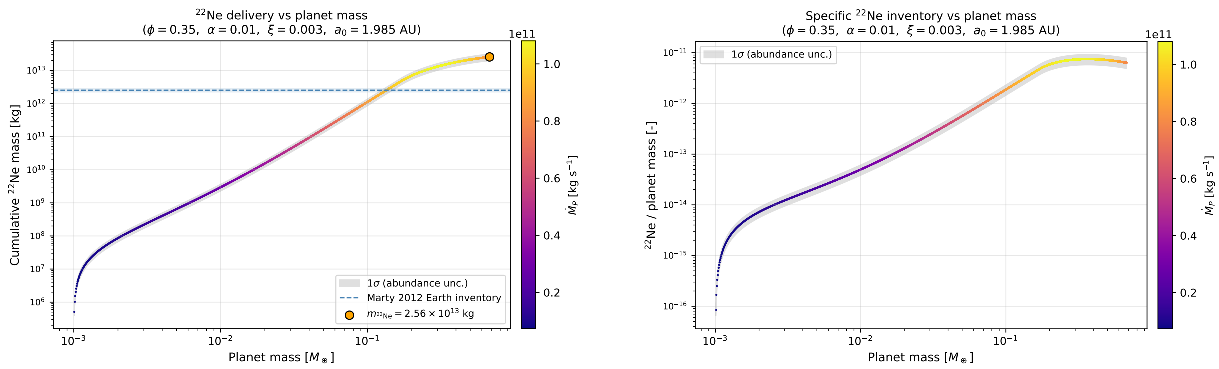

(a) (b)

Figure 6: Left (a): The cumulative amount in [kg] of $^{22}\mathrm{Ne}$ delivered during t_{PA}. A reference value taken from (Marty 2012) is included in the plot, marked by the horizontal dashed line. Right (b): The specific $^{22}\mathrm{Ne}$ delivered during the accretion time, t_{PA}. The colour of the curve is mapped to $\dot{M}_p$ in $\mathrm{kg\,s^{-1}}$, highlighting the increased gas flux to the core as M_{P} grows and the envelope temperature increases.

4 Data & Analysis

4.1 Neon and its isotope ^{22}Ne: Our model predicts that the Earth-analogous planet would accrete 2.56×10^{13} kg of ^{22}Ne through the described method over the considered, pebble accretion timescale $t_{\mathrm{PA}} = (t_{\mathrm{D}} - t_0)$ of $1.5 \times 10^6 \mathrm{yr}^{-1}$. As presented in fig. 6a, this represents an over-estimation of the combined Earth inventories (BM + ATM) as compared to the value presented by (Marty 2012). In figure 6b on the right, the specific ^{22}Ne delivery is presented, where the cumulative mass of ^{22}Ne is normalized to the mass of the planet at that point in its accretion history. A significant feature in this graph is the slanted tail beyond the point where $M_P \geq 0.2\,M_\oplus$; this shows that the diminishing $\dot{M}_g$ over time leads to a decline in pebble-assisted gas delivery as the disk begins to dissipate. In figure (5) the accretion history of ^{22}Ne produced

Table 2: Selected noble gas abundances from [Table 1.] in Marty (2012). The total Earth inventories of each isotope was found by summation and normalization of the (ATM) and (BM) concentrations to the final planet mass $0.68\,M_\oplus$.

	Solar (mol/g)	CC (mol/g)	+/-	ATM (mol/g)	BM (mol/g)	+/-
^{22}Ne	2.13E-12	1.62E-12	4.33E-13	2.27E-14	5.8E-15	3.2E-15
^{36}Ar	6.31E-13	3.47E-11	2.78E-12	9.58E-13	7.8E-14	4.3E-14
^{84}Kr	3.15E-16	4.25E-13	1.79E-14	1.98E-14	1.9E-15	1.1E-15
^{130}Xe	7.88E-18	5.38E-14	1.46E-14	1.08E-16	2.6E-17	6.8E-18

by the model for six different values of ϕ is presented. Clearly visible in the figure is that the ϕ assumed in the iterations have a large impact on the amounts of gas delivered to the protoplanetary core.

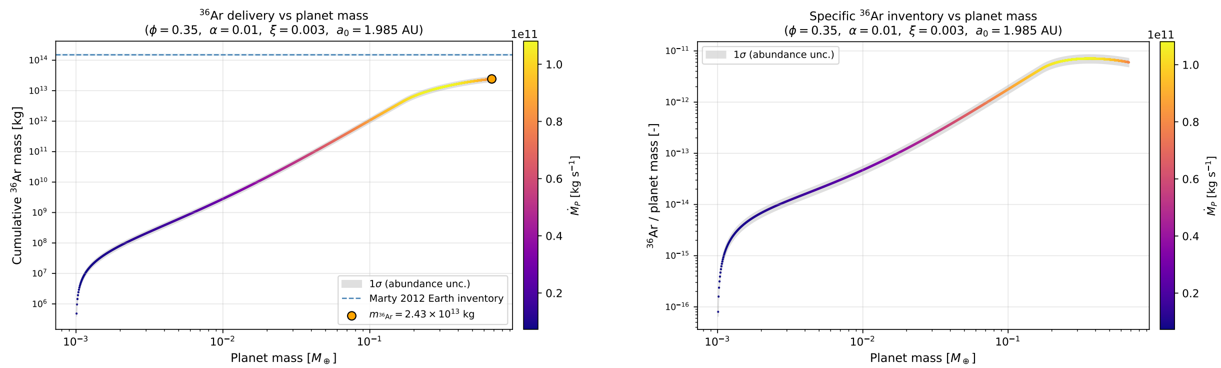

(a) (b)

Figure 7: Left (a): The cumulative amount in [kg] of $^{36}\mathrm{Ar}$ delivered during t_{PA}. A reference value taken from (Marty 2012) is included. Right (b): The specific $^{36}\mathrm{Ar}$ delivered to the protoplanet during t_{PA}.

4.2 Argon and its isotope ^{36}Ar.: Presented in figure (7a) on the left is the cumulative mass delivery of ^{36}Ar relative to the planet mass growth, and on the right in figure (7b) the specific ^{36}Ar delivery during the t_{PA} is illustrated. Compared to the terrestrial inventory presented in Marty (2012), our model delivers $\simeq 10$ times less ^{36}Ar than is measured. In part, this could be explained by the fact that the isotopic abundances in the solar system gathered from Lodders (2003) give a percentage of $\simeq 85\%$ of ^{36}Ar/Ar$_{\mathrm{total}}$, which the author notes is derived from a semi-equilibrium abundance method which is then scaled to photospheric Ar, giving a final uncertainty upon this abundance value of 20%.

The difficulty of extrapolating proto-solar abundance values for ^{36}Ar stems from the fact that ^{40}Ar is a decay product of ^{40}K, thus anchoring the uncertainty of the primordial isotopic abundance inventories of Ar to the uncertainty of the potassium inventories.

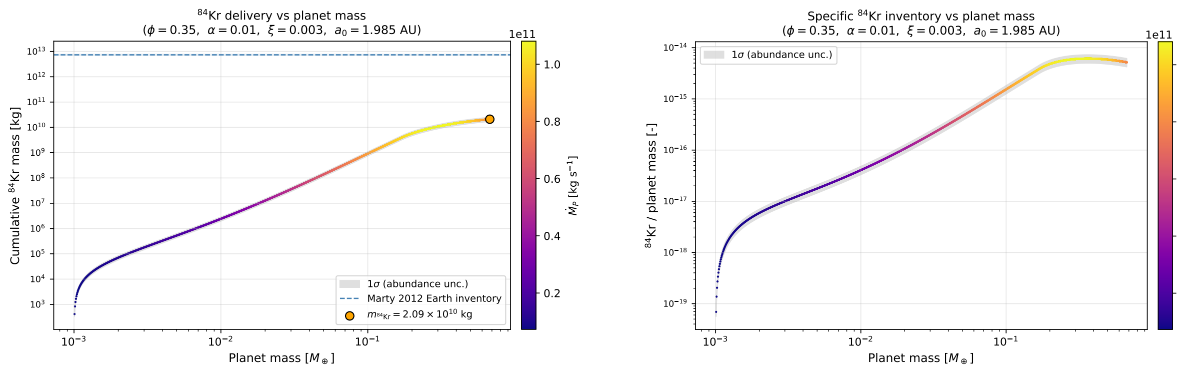

(a) (b)

Figure 8: Left (a): The cumulative amount in [kg] of $^{84}\mathrm{Kr}$ delivered during t_D. A reference value taken from (Marty 2012) is included. Right (b): The specific $^{84}\mathrm{Kr}$ delivered to the protoplanet during t_D.

4.3 Krypton and its isotope ^{84}Kr.: In figure (8a) the cumulative mass delivery of ^{84}Kr is presented. Made visible by the comparison to the terrestrial inventory from Marty (2012) is that our model drastically under-delivers ^{84}Kr. The abundances of both of the heaviest noble gases Kr and Xe considered here in the primordial inventories were again collected from Lodders (2003). Both of these inventories were based on neutron-element systematics, which the author specifies as yielding a higher elemental abundance than earlier works (see sect. 2.3.1.4 in Lodders (2003)). Our model, using these elemental abundances, nevertheless gives roughly 4 orders-of-magnitude less accreted ^{84}Kr-mass than is measured by Marty (2012).

4.4 Xenon and its isotope ^{130}Xe.: Presented in figure (9a) is the accumulated mass of ^{130}Xe during t_PA. As in the case for ^{84}Kr our model once more calculates a significantly lower accreted ^{130}Xe inventory than is measured in Marty (2012). The difference is slightly smaller than in the case of ^{84}Kr, representing an approximate depletion on the order of 2.6×10^2 kg relative to the reference value.

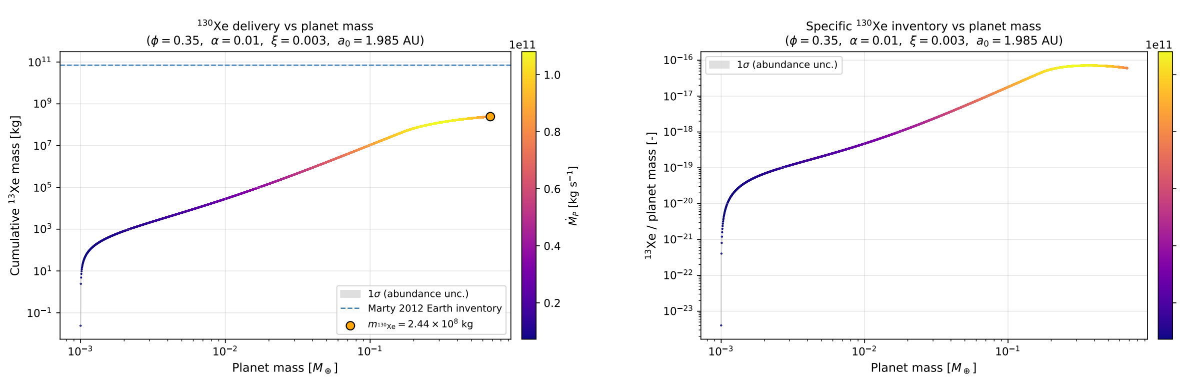

(a) (b)

Figure 9: Left (a): The cumulative amount in [kg] of $^{130}\mathrm{Xe}$ delivered during t_D. A reference value taken from (Marty 2012) is included. Right (b): The specific $^{130}\mathrm{Xe}$ delivered to the protoplanet during t_D.

This presents a reversal of the trend observed in the previous three cases, as the gap between the predicted mass-values and the respective inventory reference values from Marty (2012) can be observed to increase for the heavier isotopes. Likely, this illustrates the fact that the reference value reflects the well-known Xe$-$paradox, where the Earths inventory of Xe is severely depleted in lighter isotopes e.g. ^{129}Xe in comparison to both the solar-wind and chondritic abundance measurements, and without this paradox our result could feasibly show a continuation in the trend of exacerbating the disparity between the model calculated value and the reference inventories.

5 Discussion

The results of the model show that pebble accretion may plausibly deliver some amounts of noble gases from the protoplanetary disk into the forming core, under the present assumed conditions. As presented in fig. (5) however, the delivery is greatly dependent on the ϕ-parameter, which is not yet well defined for pebbles forming within the model. While the assumed St gives an idea of the aerodynamical sizes of pebbles which can be converted to a physical size via (eq. 21), the model does not include the formation history of pebbles. Without determining an analytic expression which can describe how the filling factor of pebbles manifests, the best results this model is an exploration of the effect of different levels of porosity. The filling factor could conceivably change with time, disk temperature or radial distance within the disk, as the evolving disk temperature and positions of the snow lines affect the stickiness of monomers and thus the filling factor ϕ.

Under the assumptions of constant pebble sizes and densities, as well as an unchanging disk elemental composition, the effects of the migration of the planet into the model will only have a modest effect on our results. To gain a more accurate image of the possibility of pebbles as vehicles for gas transport, further development of the model is needed. Some identified areas where the model could be improved upon would be including some degree of accretion of (Marty (2012)), contributions from comets e.g. during the hypothesized *late veneer* accretion stage (Bouhifd et al. (2020)) and the effects of solar wind which Avice et al. (2022) argue could explain the $^{20}\mathrm{Ne}/^{22}\mathrm{Ne}$ ratio of Venus' atmosphere. The solar wind has been shown to contain an enhanced concentration of heavier isotopes of lighter elements (Heber et al. (2009)) as a consequence of mass-dependent isotopic fractionation.

Our model uses the recommended proto-solar abundances from Lodders (2003), and we make no attempt at modeling the chemical evolution of the gaseous material in the disk at different times or distance to the central star during our planets migration. This is likely not a completely accurate representation of the true chemical conditions of the disk gas as there is no evidence, known to the author at the present, to suggest that the elemental composition of gas in the disk would be initially, and remain for the entirety of the t_{D}, homogeneous. While noble gases are inert, and thus their abundances within the disk gas will not change due to chemical interactions such as forming molecules, by which one can surmise that a solar mixing ratio of, for instance, Ne relative to $\mathrm{H_2}$ and He, The reason for taking to be $\simeq 1\,\mathrm{cm}$ is explained in section [**3.3**], however, this is built upon the assumption that the Stokes number of the pebbles remains static throughout the disk evolution. As St is in essence a free parameter within the model, however we note that recent evidence suggests St ought to be constrained to within the range $0.01 \sim 0.03$ (cf. Jiang, Haochang et al. (2024)), a reasonable question an observant reader may have is what our results would show if one assumes a different Stokes number. In addition to determining R_{peb}, the value of St contributes to determining the efficiency of planet growth in equation (10), which itself contains a parameterization of the solid-mass flux rate $\dot{M}_{\mathrm{p}}$, expressed as $\dot{M}_{\mathrm{p}} = \xi\,\dot{M}_{\mathrm{g}}$. This means that naively changing the St value of the pebbles without computing how this affects the radial drift speed v_r of the particles within the disk which sets the mass fluxes $\dot{M}_{\mathrm{g}}$ and $\dot{M}_{\mathrm{p}}$, where $v_r = -\frac{2\Delta v}{\mathrm{St}+\mathrm{St}^{-1}} + \frac{u_r}{1+\mathrm{St}^2}$ (Johansen et al. (2019)), will have wide spread implications upon the migration history of our planet. Spectrometric evidence from other disks suggest that PPDs contain large reservoirs of solids of sizes in the micrometer to millimeter range (Hartmann et al. (1998)), and several studies point to the fact that the growth barriers that hinder the growth of pebble sizes are alleviated beyond the water- or CO-snow lines (e.g Gonzalez and Michoulier (2026); Price et al. (2021)), perhaps hinting that the average size of solids within the disk could develop over the lifetime of the disk. However, except for the change in the V_{tot} of the pebbles via (eq. 21 , 27), the St-value does not explicitly set the gas accretion rate onto the protoplanet. As the parameters constraining ϕ are not yet well understood, using a static $\mathrm{St} = 0.01$ will not, by itself, constrain our model in a meaningful way.

Without accounting for the mass contributions of chondrites, comets, or the moon forming giant impact, the results of the model may only serve as a proof of concept of the mechanism of porous pebbles as carriers of primordial gas into the magmatic ocean of the forming protoplanet. However, there is evidence which lends credibility to the theory that some amount of disk gas must be delivered into the silicate core during the formation of the planet. Several works within the field of geochemistry have presented their deductions regarding the contributions of e.g. carbonaceous chondrites in order to explain the isotopic abundance ratios measured in Earths atmosphere and mantle (Marty (2012) ; Bouhifd et al. (2020) ; Öberg and Bergin (2021)), which describe a solar component of gas present within the Earths mantle as an, as of yet, unanswered question.

The crux of the problem, laid out in Marty (2012) and discussed at length in Bouhifd et al. (2020), is that the inertness and low solubility of noble gases in silicates suggests that at high pressures these reservoirs ought not to be retained within the solid mass of the Earth as the supercritical magmatic ocean cooled, and would be quickly degassed once the mantle crystallizes. However, the measured abundances within mid-ocean ridge basalts and other surface inventories do not reflect these conclusions, as recent surveys have detected a solar component emanating from the Earth (Bouhifd et al. (2020)).

Calculating the amounts of diffused gas from the magmatic ocean into the envelope falls outside the scope of this project, and we make no attempt at estimating these amounts. Instead, we opt to include the full concentrations of the selected isotopes in both the atmosphere and the bulk mantle as presented by Marty (2012), yet make no attempt at including the concentrations of these gases from within the envelope. This is a potential source of error in our final results, as we do not account for the retention of gases from the envelope as it contracts and forms an eventual atmosphere. Our reasoning for this is due to the substantial uncertainties regarding the effects of fractionation during envelope outgassing and hydrodynamic recycling between the surrounding disk material (Jakosky et al. (1994)).

As discussed by Öberg and Bergin (2021), the combined chemical records of solar system objects suggest that the protoplanetary disk underwent both a chemical reset, where complex molecules are dissociated and their materials are spread within the disk material, and displays clear inheritance as the outer disk temperature is remarkably low temperature, allowing the preservation of pristine chemical signatures within ices in the outer disk.

A natural extension of this model would thus be to incorporate the chemical evolution of the disk material with respect to time and semi-major axis a, which would need to incorporate an expression for the recycling flows between the disk and outer parts of the envelope. Ideally, such a model would also include the effects of fractionation in hydrodynamical escape processes, the intricacies of which is still being investigated (see e.g. Valatsou et al. (2026)) as pertaining to the escape of gas from the envelope.

Another process that we do not account for in the model is the mass-loss rate of pebbles during their accretion. In reality, the ablation and compactification of highly porous pebbles ($\phi \to 0.01$) would likely be significant during their infall through the envelope (Schneider, Niclas and Wurm, Gerhard (2021)) as the Van der Waal's forces adhering the grains in the pebbles are extremely fragile (Ali-Dib and Thompson (2020)). Such processes could lower the gas volume-fraction held within the pebbles, a volume that the current model assumes to be constant and has widespread implications for the total gas mass delivered during the pebble accretion process.

As discussed in Paszun, D. and Dominik, C. (2009), while collisions of highly porous aggregates within the disk may effectively lead to mass transfer or growth via "*hit-and-stick*" collisions at low velocities (cf. Zsom et al. (2010) ; Drażkowska et al. (2019)), the binding energy between constituent grains is low, even accounting for the increased stickiness of ice pebbles. It thus stands to reason that the drag forces experienced by the incident pebbles would likely contribute to some degree of compactification, the inclusion of which would be a natural extension of the model.

6 Conclusions

6.1 Results of gas accretion in pebbles: Our model uses constant pebble sizes of $1\,\mathrm{cm}$ and a sublimation temperature T_S of $1500\,\mathrm{K}$ for a range of filling factors ϕ, choosing to present the main results using a nominal value of $\phi = 0.35$ based on the conclusions of Blum and Wurm (2008). We use the model of pebble accretion laid out in Steinmeyer et al. (2023) to calculate the planetary growth and migration track, the conditions of the PPD and the hydrodynamical profiles of the protoplanetary envelope.

By incorporating the projections of proto-solar elemental abundances laid out in Lodders (2003), and collecting a reference value for the combined Earth inventories, contained within the atmosphere and bulk mantle, of four select isotopes of noble gases from Marty (2012) we model the cumulative and specific accretion histories of these four isotopes delivered within porous pebbles. The results of the model reflect an over-delivery of the lightest noble gas isotope considered, ^{22}Ne, while delivering substantially less of the heavier isotopes of ^{36}Ar, ^{84}Kr and ^{130}Xe. The observed trend is that the disparity between the measured Earth inventories and cumulative amounts of gas delivered via pebble accretion appears to be increasing, especially when accounting for the observed lack of Xe in the Earth's inventories known as the Xe-paradox. The results, meanwhile, do point to a possible explanation for the long standing problem regarding the observed solar composition of terrestrial Ne, and the isotopic compositions of the heavier noble gases could likely be explained by incorporating the contributions of carbonaceous chondrites.

The question which motivated the project was whether pebbles could conceivably act as a vehicle for delivery of gas from the PPD down into the magmatic ocean constituting the surface of the forming protoplanet. Interpreting the results proved quite a difficult task, as there are a large number of factors regarding which there does not yet exist a widespread scientific consensus, such as the mass and accompanying elemental contributions of chondrites, meteorites or comets during a theorized late veneer epoch of core formation. Additionally, the prevailing theory behind how the Earth-Moon system formed describes a giant impact between the proto-Earth and another object, during which a considerable amount of mass transfer is presumed to have occurred (Yu and Jacobsen (2011) ; Lock et al. (2018)), which likely contributed a considerable amount of solid mass to the proto-Earth core which would have had been accreted under different chemical conditions. These types of ballistic impacts would also contribute to a degassing of the solid surface material of the core (Avice et al. (2022)) which is difficult to account in this model.

The conclusion to be drawn from these results is that the model may serve as a proof-of-concept, that likely some amount of gas is transported into the protoplanetary core during the pebble accretion process. While the model clearly does not provide a self-sufficient, stand-alone, explanation for the isotopic abundances of noble gases of the Earth analogue in this iteration, the project still produces valuable insights into a number of limitations regarding the viability of pebbles as vehicles for gaseous transport. We find that the filling factor ϕ plays a vital role in determining the amount of accreted gas. However, without taking the chemical evolution of the disk gas into account, over time and with respect to the distance to the central star, merely varying the ϕ-factor would not change the relative abundances of the investigated noble gas isotopes, as even an increased gas mass delivery from the static-composition disk gas, e.g. by letting $\phi \to 0$, would still perpetuate the same relationship between the cumulative amounts of the four noble gases.

6.2 Outlook and considerations for developing the model: In future modeling of the mechanism of gas accretion via pebble accretion, a method of evaluating the chemical development of the disk material ought to be included. As the outer reaches of the envelope is presumed to be in physical contact with the disk material, and due to the recycling flows occurring between the envelope and the disk material, this will greatly affect the chemical abundances available for transport within pebbles over time.

Additionally, as chondritic samples show a considerable amount of fractionation of included gaseous material, assumedly there are processes within which chondrites form, and in the hydrodynamical escape from the envelope, where isotopic fractionation should be considered in the disk material which constitute both the pebbles and the gas supplied to the envelope which is not accounted for in this iteration of the model. While accounting for fractionation in all these processes could prove beyond the realm of possibility, a natural extension of the model would be to include the contributions of carbonaceous chondrites. The goal of such a project could then be to understand how large of a contribution of carbonaceous chondrites, supplemented by the contributions from porous pebbles described in this project, is required to adequately explain the isotopic compositions of noble gases found in the Earths inventories.

Lastly, estimating the mass contributions of other categories of solids during the formation process of the protoplanetary core would be of monumental importance if the model is to be able to produce accurate predictions.

References

M. Ali-Dib and C. Thompson. Limits on Protoplanet Growth by Accretion of Small Solids. , 900 (2):96, Sept. 2020. doi: 10.3847/1538-4357/aba521.

P. J. Armitage. *Planet Formation Theory: An Overview*, pages 1–41. Springer Nature Switzerland, Cham, 2017. ISBN 978-3-319-30648-3. doi: 10.1007/978-3-319-30648-3_135-2. URL https://doi.org/10.1007/978-3-319-30648-3_135-2.

G. Avice, R. Parai, S. Jacobson, J. Labidi, M. G. Trainer, and M. P. Petkov. Noble gases and stable isotopes track the origin and early evolution of the venus atmosphere. *Space Science Reviews*, 218(8):60, 2022. ISSN 1572-9672. doi: 10.1007/s11214-022-00929-9. URL https://doi.org/10.1007/s11214-022-00929-9.

K. R. Bell and D. N. C. Lin. Using FU Orionis Outbursts to Constrain Self-regulated Protostellar Disk Models. , 427:987, June 1994. doi: 10.1086/174206.

E. A. Bergin, L. I. Cleeves, U. Gorti, K. Zhang, G. A. Blake, J. D. Green, S. M. Andrews, N. J. Evans II, T. Henning, K. Öberg, K. Pontoppidan, C. Qi, C. Salyk, and E. F. van Dishoeck. An old disk still capable of forming a planetary system. *Nature*, 493(7434):644–646, 2013. ISSN 1476-4687. doi: 10.1038/nature11805. URL https://doi.org/10.1038/nature11805.

T. Birnstiel, M. Fang, and A. Johansen. Dust evolution and the formation of planetesimals. *Space Science Reviews*, 205(1):41–75, 2016. ISSN 1572-9672. doi: 10.1007/s11214-016-0256-1. URL https://doi.org/10.1007/s11214-016-0256-1.

D. Black and R. Pepin. Trapped neon in meteorites — ii. *Earth and Planetary Science Letters*, 6(5):395–405, 1969. ISSN 0012-821X. doi: https://doi.org/10.1016/0012-821X(69)90190-3. URL https://www.sciencedirect.com/science/article/pii/0012821X69901903.

J. Blum and R. Schräpler. Structure and Mechanical Properties of High-Porosity Macroscopic Agglomerates Formed by Random Ballistic Deposition. , 93(11):115503, Sept. 2004. doi: 10.1103/PhysRevLett.93.115503.

J. Blum and G. Wurm. The growth mechanisms of macroscopic bodies in protoplanetary disks. , 46:21–56, Sept. 2008. doi: 10.1146/annurev.astro.46.060407.145152.

M. A. Bouhifd, A. P. Jephcoat, D. Porcelli, S. P. Kelley, and B. Marty. Potential of earth's core as a reservoir for noble gases: Case for helium and neon. *Geochemical Perspectives Letters*, 15:15–18, 2020. doi: 10.7185/geochemlet.2028. URL https://www.geochemicalperspectivesletters.org/article2028.

J. Drazkowska, B. Bitsch, M. T. A. Lambrechts, G. D. Mulders, D. Harsono, A. Vazan, B. Liu, C. W. Ormel, K. Kretke, and A. Morbidelli. Planet formation theory in the era of alma and kepler: from pebbles to exoplanets. Workingpaper, arXiv.org, 2022.

J. Drażkowska, S. Li, T. Birnstiel, S. M. Stammler, and H. Li. Including dust coagulation in hydrodynamic models of protoplanetary disks: Dust evolution in the vicinity of a jupiter-mass planet. *The Astrophysical Journal*, 885(1):91, nov 2019. doi: 10.3847/1538-4357/ab46b7. URL https://doi.org/10.3847/1538-4357/ab46b7.

Franceschi, Riccardo, Birnstiel, Tilman, Henning, Thomas, Pinilla, Paola, Semenov, Dmitry, and Zormpas, Apostolos. Mass determination of protoplanetary disks from dust evolution. *A&A*, 657:A74, 2022. doi: 10.1051/0004-6361/202141705. URL https://doi.org/10.1051/0004-6361/202141705.

J.-F. Gonzalez and S. Michoulier. The CO snow line favours strong clumping by the streaming instability in protoplanetary discs with porous grains. , 706:L14, Feb. 2026. doi: 10.1051/0004-6361/202557914.

L. Hartmann, N. Calvet, E. Gullbring, and P. D'Alessio. Accretion and the evolution of t tauri disks. *The Astrophysical Journal*, 495:385–400, March 1998.

V. S. Heber, R. Wieler, H. Baur, C. Olinger, T. A. Friedmann, and D. S. Burnett. Noble gas composition of the solar wind as collected by the genesis mission. *Geochimica et Cosmochimica Acta*, 73(24):7414–7432, 2009. ISSN 0016-7037. doi: https://doi.org/10.1016/j.gca.2009.09.013. URL https://www.sciencedirect.com/science/article/pii/S0016703709005833.

D. Hughes. The mean density of the Earth. *Journal of the British Astronomical Association*, 116 (1):21, Feb. 2006.

B. M. Jakosky, R. O. Pepin, R. E. Johnson, and J. L. Fox. Mars Atmospheric Loss and Isotopic Fractionation by Solar-Wind-Induced Sputtering and Photochemical Escape. , 111(2):271–288, Oct. 1994. doi: 10.1006/icar.1994.1145.

Jiang, Haochang, Macías, Enrique, Guerra-Alvarado, Osmar M., and Carrasco-González, Carlos. Grain-size measurements in protoplanetary disks indicate fragile pebbles and low turbulence. *A&A*, 682:A32, 2024. doi: 10.1051/0004-6361/202348271. URL https://doi.org/10.1051/0004-6361/202348271.

A. Johansen and M. Lambrechts. Forming planets via pebble accretion. *Annual Review of Earth and Planetary Sciences*, 45(Volume 45, 2017):359–387, 2017. ISSN 1545-4495. doi: https://doi.org/10.1146/annurev-earth-063016-020226. URL https://www.annualreviews.org/content/journals/10.1146/annurev-earth-063016-020226.

A. Johansen and W. Lyra. Exploring the conditions for forming planetesimals by the streaming instability and planetary systems by pebble accretion, 2026. URL https://arxiv.org/abs/2604.25816.

A. Johansen and A. Youdin. Protoplanetary Disk Turbulence Driven by the Streaming Instability: Nonlinear Saturation and Particle Concentration. , 662(1):627–641, June 2007. doi: 10.1086/516730.

A. Johansen, J. S. Oishi, M. M. M. Low, H. Klahr, T. Henning, and A. Youdin. Rapid planetesimal formation in turbulent circumstellar disks. *Nature*, 448(7157):1022–1025, 2007. doi: 10.1038/nature06086.

A. Johansen, M.-M. Mac Low, P. Lacerda, and M. Bizzarro. Growth of asteroids, planetary embryos, and Kuiper belt objects by chondrule accretion. *Science Advances*, 1:1500109, Apr. 2015. doi: 10.1126/sciadv.1500109.

A. Johansen, S. Ida, and R. Brasser. How planetary growth outperforms migration. , 622:A202, Feb. 2019. doi: 10.1051/0004-6361/201834071.

Johansen, Anders, Ronnet, Thomas, Schiller, Martin, Deng, Zhengbin, and Bizzarro, Martin. Anatomy of rocky planets formed by rapid pebble accretion - i. how icy pebbles determine the core fraction and feo contents. *A&A*, 671:A74, 2023. doi: 10.1051/0004-6361/202142141. URL `https://doi.org/10.1051/0004-6361/202142141`.

R. Kippenhahn, A. Weigert, and A. Weiss. *Stellar Structure and Evolution*. Astronomy and Astrophysics Library. Springer Berlin Heidelberg, 2 edition, 2012. ISBN 978-3-642-30304-3. doi: 10.1007/978-3-642-30304-3. URL `https://doi.org/10.1007/978-3-642-30304-3`.

M. Lambrechts, A. Johansen, and A. Morbidelli. Separating gas-giant and ice-giant planets by halting pebble accretion. , 572:A35, Dec. 2014. doi: 10.1051/0004-6361/201423814.

G. Lesur, M. W. Kunz, and S. Fromang. Thanatology in protoplanetary discs: dead zones and the role of non-ideal mhd. *Astronomy & Astrophysics*, 566:A56, 2014. doi: 10.1051/0004-6361/201423660.

S. J. Lock, S. T. Stewart, M. I. Petaev, Z. Leinhardt, M. T. Mace, S. B. Jacobsen, and M. Cuk. The Origin of the Moon Within a Terrestrial Synestia. *Journal of Geophysical Research (Planets)*, 123(4):910–951, Apr. 2018. doi: 10.1002/2017JE005333.

K. Lodders. Solar system abundances and condensation temperatures of the elements. *The Astrophysical Journal*, 591(2):1220, jul 2003. doi: 10.1086/375492. URL `https://doi.org/10.1086/375492`.

F. Long, P. Pinilla, G. J. Herczeg, I. Pascucci, C. F. Manara, N. Hendler, G. Lodato, L. Testi, and A. Natta. Observational signatures of dust trapping in protoplanetary disks. *The Astrophysical Journal*, 882:49, 2019. doi: 10.3847/1538-4357/ab2d2d.

C. F. Manara, M. Ansdell, G. P. Rosotti, and et al. Protostars and planets vii contribution. In *Protostars and Planets VII*, volume 534 of *ASP Conference Series*, page 539. Astronomical Society of the Pacific, 2023.

B. Marty. The origins and concentrations of water, carbon, nitrogen and noble gases on earth. *Earth and Planetary Science Letters*, 313-314:56–66, 2012. ISSN 0012-821X. doi: https://doi.org/10.1016/j.epsl.2011.10.040. URL `https://www.sciencedirect.com/science/article/pii/S0012821X11006388`.

S. Michoulier, J.-F. Gonzalez, and D. J. Price. Compaction during fragmentation and bouncing produces realistic dust grain porosities in protoplanetary discs. , 688:A31, Aug. 2024. doi: 10.1051/0004-6361/202449719.

Mordasini, C. Grain opacity and the bulk composition of extrasolar planets - ii. an analytical model for grain opacity in protoplanetary atmospheres. *A&A*, 572:A118, 2014. doi: 10.1051/0004-6361/201423702. URL `https://doi.org/10.1051/0004-6361/201423702`.

S. Mori, S. Okuzumi, M. Kunitomo, and X.-N. Bai. Evolution of the Water Snow Line in Magnetically Accreting Protoplanetary Disks. , 916(2):72, Aug. 2021. doi: 10.3847/1538-4357/ac06a9.

G. D. Mulders, I. Pascucci, C. F. Manara, L. Testi, G. J. Herczeg, T. Henning, S. Mohanty, and G. Lodato. Constraints from Dust Mass and Mass Accretion Rate Measurements on Angular Momentum Transport in Protoplanetary Disks. , 847(1):31, Sept. 2017. doi: 10.3847/1538-4357/aa8906.

K. I. Öberg and E. A. Bergin. Astrochemistry and compositions of planetary systems. , 893: 1–48, Jan. 2021. doi: 10.1016/j.physrep.2020.09.004.

S. Okuzumi, H. Tanaka, H. Kobayashi, and K. Wada. Rapid Coagulation of Porous Dust Aggregates outside the Snow Line: A Pathway to Successful Icy Planetesimal Formation. , 752(2):106, June 2012. doi: 10.1088/0004-637X/752/2/106.

C. Ormel. An atmospheric structure equation for grain growth. *The Astrophysical Journal Letters*, 789(1):L18, jun 2014. doi: 10.1088/2041-8205/789/1/L18. URL `https://doi.org/10.1088/2041-8205/789/1/L18`.

C. W. Ormel, R. Kuiper, and J.-M. Shi. Hydrodynamics of embedded planets' first atmospheres – i. a centrifugal growth barrier for 2d flows. *Monthly Notices of the Royal Astronomical Society*, 446(1):1026–1040, 01 2015. ISSN 0035-8711. doi: 10.1093/mnras/stu2101. URL `https://doi.org/10.1093/mnras/stu2101`.

M. Ozima and F. A. Podosek. *Noble Gas Geochemistry*. Cambridge University Press, 2 edition, 2001.

Paszun, D. and Dominik, C. Collisional evolution of dust aggregates. from compaction to catastrophic destruction. *A&A*, 507(2):1023–1040, 2009. doi: 10.1051/0004-6361/200810682. URL `https://doi.org/10.1051/0004-6361/200810682`.

E. M. Price, L. I. Cleeves, D. Bodewits, and K. I. Öberg. Ice-coated Pebble Drift as a Possible Explanation for Peculiar Cometary CO/H_2O Ratios. , 913(1):9, May 2021. doi: 10.3847/1538-4357/abf041.

U. Schäfer, C. Yang, and A. Johansen. Initial mass function of planetesimals formed by the streaming instability. *Astronomy and Astrophysics*, 597, Jan. 2017. ISSN 0004-6361. doi: 10.1051/0004-6361/201629561.

Schneider, Niclas and Wurm, Gerhard. Drag forces on porous aggregates in protoplanetary disks. *A&A*, 655:A50, 2021. doi: 10.1051/0004-6361/202141582. URL https://doi.org/10.1051/0004-6361/202141582.

N. I. Shakura and R. A. Sunyaev. Black holes in binary systems. observational appearance. *Astronomy and Astrophysics*, 24:337–355, 1973.

J. B. Simon, P. J. Armitage, R. Li, and A. N. Youdin. The Mass and Size Distribution of Planetesimals Formed by the Streaming Instability. I. The Role of Self-gravity. , 822(1):55, May 2016. doi: 10.3847/0004-637X/822/1/55.

M.-L. Steinmeyer and A. Johansen. Vapor equilibrium models of accreting rocky planets demonstrate direct core growth by pebble accretion. *A&A*, 683:A217, 2024. doi: 10.1051/0004-6361/202349052. URL https://doi.org/10.1051/0004-6361/202349052.

M.-L. Steinmeyer, P. Woitke, and A. Johansen. Sublimation of refractory minerals in the gas envelopes of accreting rocky planets. , 677:A181, Sept. 2023. doi: 10.1051/0004-6361/202245636.

M. Valatsou, C. Dorn, P. Marty, and J. E. Owen. Oxygen left behind: Atmospheric enrichment due to fractionation in sub-neptunes using boreas. *The Astrophysical Journal*, 1002:53, 2026. doi: 10.3847/1538-4357/ae5104.

R. G. Visser and C. W. Ormel. On the growth of pebble-accreting planetesimals. , 586:A66, Feb. 2016. doi: 10.1051/0004-6361/201527361.

A. N. Youdin and J. Goodman. Streaming Instabilities in Protoplanetary Disks. , 620(1):459–469, Feb. 2005. doi: 10.1086/426895.

G. Yu and S. B. Jacobsen. Fast accretion of the Earth with a late Moon-forming giant impact. *Proceedings of the National Academy of Science*, 108(43):17604–17609, Oct. 2011. doi: 10.1073/pnas.1108544108.

A. Zsom, C. W. Ormel, C. Güttler, J. Blum, and C. P. Dullemond. The outcome of protoplanetary dust growth: pebbles, boulders, or planetesimals? II. Introducing the bouncing barrier. , 513: A57, Apr. 2010. doi: 10.1051/0004-6361/200912976.